three power inputs; 20, 5, and 1 mw peak. The fine structure, particularly evident in the 20-mw curve, is related to the standing wave ratio of the microwave line. At points of poorer matching (*i.e.*, at 3000 and 3400 Mc), the incident power upon the detector is diminished, with a consequent lowering of the amount of light quenching.

The Future of the Plasma Detector

The plasma microwave detector, as it exists today, does not rival the crystal rectifier as an envelope detector. A standard crystal rectifier can detect signals with strengths in the order of 10^{-8} watts. In the present state of development, the plasma detector under optimum conditions can respond to about 10^{-6} watts of incident energy. A crystal semiconductor used as a mixer can detect microwave signals as small as 10^{-13} watts. The plasma microwave detector has not been investigated for any mixing properties.

There are, however, several approaches available to improve the present minimum detectable signal level. An obvious method of increasing the plasma detector sensitivity is to employ a dc magnetic field so as to cause the plasma electrons to execute cyclotron motion. In this condition, the electrons are more efficient absorbers of microwave energy at particular microwave frequencies, and will produce more profound quenching of light output. The relationship of magnetic field to applied microwave frequency may be related simply by $B=0.357f$, where B is the magnetic field in Gauss and f is the applied microwave frequency in Mc per second. Thus, to produce maximum signal enhancement at 3000 Mc, a 1070-Gauss magnetic field would be employed. Such operation will narrow the bandwidth of the device.

Practical difficulties may prevent full utilization of the advantages expected from operation at cyclotron resonance. These difficulties concern the compromise necessary in optimum gas pressure to satisfy the conflicting requirements of minimizing pressuring broadening effects on cyclotron resonance, maintaining a stable discharge, and minimizing unwanted electron loss through diffusion. The magnetic field required for cyclotron resonance, however, yields the advantage of restraining electron diffusion.

Methods to enhance or multiply the incident microwave signal offer other sensitivity increasing techniques. The use of "squeezed" waveguide sections, resonant cavities, and similar structures effectively multiplies the incident power density upon the detector. These manipulations also narrow the bandwidth of operation.

Finally, it should be remembered that we can measure only what we can see. The present method of display, presentation, and observation leaves much to be desired as far as determining the ultimate sensitivity of this device.

Interaction of a Modulated Electron Beam with a Plasma*

G. D. BOYD†, MEMBER, IRE, R. W. GOULD‡, MEMBER, IRE, AND L. M. FIELD||, FELLOW, IRE

Summary—**The results of a theoretical and experimental investigation of the high-frequency interaction of an electron beam with a plasma are reported. An electron beam, modulated at a microwave frequency, passes through a uniform region of a mercury arc discharge after which it is demodulated. Exponentially growing wave amplification along the electron beam was experimentally observed for the first time at a microwave frequency equal to the plasma frequency. Approximate theories of the effects of 1) plasma-electron collision frequencies, 2) plasma-electron thermal velocities and 3) finite beam diameter, are given.**

In a second experiment the interaction between a modulated electron beam and a slow electrostatic wave on a plasma column has been studied. A strong interaction occurs when the velocity of the electron beam is approximately equal to the velocity of the wave and the interaction is essentially the same as that which occurs in traveling-wave amplifiers, except that here the plasma colum replaces the usual helical slow-wave circuit. The theory predicting rates of growth is presented and compared with the experimental results.

* Received by the IRE, August 7, 1961. This work was supported by the Office of Naval Research, Contract NONR 220(13).
† Bell Telephone Labs., Inc., Murray Hill, N. J.
‡ California Inst. of Tech., Pasadena, Calif.
|| Microwave Tube Div., Hughes Aircraft Co., Culver City, Calif.

I. Introduction

In 1929 Tonks and Langmuir[1] reported on experiments involving electron-plasma oscillations and defined the electron-plasma oscillation frequency

$$\omega_p^2 = \frac{n_0 e^2}{m\epsilon_0} \tag{1}$$

where e is the magnitude of the electronic charge, m its mass, n_0 the density of plasma electrons per unit volume, and ϵ_0 the permittivity of free space. (MKS units are used throughout this paper.)

When the electron thermal velocities are small compared to the velocity of waves being considered, the plasma can be characterized by a dielectric constant

$$\frac{\epsilon}{\epsilon_0} = 1 - \frac{\omega_p^2}{\omega(\omega - i\nu)}, \tag{2}$$

where ω is the angular signal frequency and ν is an effective collision frequency for the plasma electrons. For the experiments described in this paper the effect of the massive positive ions may be neglected.

In 1948 Haeff[2] suggested that plasma oscillations excited by a directed beam of charged particles might be responsible for certain types of RF energy received from the sun, and he discussed the mechanism of two-stream amplification. Bohm and Gross[3] have given a more extensive discussion of the interaction of an electron beam and a thermal plasma. Complex propagation constants were found for waves whose frequency is approximately equal to the plasma frequency defined in (1). The significance of the complex propagation constant is that small disturbances are amplified as the beam drifts through the plasma. In an earlier paper Pierce[4] had noticed a similar instability when an electron beam passed through a positive ion cloud and had attempted to relate this to positive ion oscillations observed in vacuum tubes. These discoveries have stimulated a very great amount of theoretical study of instabilities in plasmas with non-Maxwellian velocity distribution. The amplification mechanism, however, is essentially that of the double-stream amplifier invented by Haeff[5] and independently by Pierce and Hebenstreit.[6] In the case of the plasma, one group of charged particles is stationary.

Several experiments have been performed in which directed electron beams are passed through the plasma region of a gas discharge. Looney and Brown's[7] early experiment is representative. A beam of high-energy electrons (several hundred volts) was injected into the plasma of a dc discharge from an auxiliary electron gun. RF signals were detected by a small wire probe placed in the beam. The probe was movable and showed the existence of standing-wave patterns of oscillatory energy. Nodes of the pattern coincided with electrodes which bound the plasma. The thickness of the ion sheaths at these electrodes determined the standing-wave pattern. The frequencies of oscillation seemed to be related to the transit time effects of the electrons between the sheaths and did not appear to verify the theory of Bohm and Gross.[3] Later Gordon[8] investigated the energy exchange mechanism which was involved and showed that the results of Looney and Brown might be understood in terms of reflex klystron oscillations due to the electron beam being reflected by the sheaths. He found that the radiation detected by the probe was due to the fields of the bunched beam and not primarily due to plasma oscillations. Wehner[9] had previously built a plasma oscillator using this klystron bunching principle.

Very recently Kofoid[10] found oscillations very similar to those of Looney and Brown when two oppositely directed electron beams were passed through the plasma. This result tends to support Gordon's conclusion.

The dispersion equation for small amplitude waves in a system consisting of a beam and a collisionless plasma has been derived by a number of investigators.

$$1 = \frac{\omega_p^2}{\omega^2} + \frac{\omega_b^2}{(\omega - \gamma v_b)^2} \tag{3}$$

where ω_p is the plasma frequency of the plasma, ω_b is the plasma frequency of the beam, and v_b is the drift velocity of the beam. A number of simplifying assumptions have been made in obtaining this result:

1) Only small sinusoidal waves have been considered.
2) The electric vector and the direction of propagation of waves have been taken parallel to the direction of the beam (longitudinal waves).
3) All quantities were independent of the coordinates

[1] L. Tonks and I. Langmuir, "Oscillations in ionized gases," *Phys. Rev.*, vol. 33, pp. 195, 990; 1929.
[2] A. V. Haeff, "Space-charge wave amplification effects," *Phys. Rev.*, vol. 74, pp. 1532–1533; 1948. Also, "On the origin of solar radio noise," *Phys. Rev.*, vol. 75, pp. 1546–1551; 1949.
[3] D. Bohm and E. P. Gross, "Theory of plasma oscillations. A. Origin of medium-like behavior," *Phys. Rev.*, vol. 75, pp. 1851–1864; 1949. Also, "Theory of plasma oscillations. B. Excitation and damping of oscillations," *Phys. Rev.*, vol. 75, pp. 1864–1876; 1949. Also, "Effects of plasma boundaries in plasma oscillations," *Phys. Rev.*, vol. 79, pp. 992–1001; 1950.
[4] J. R. Pierce, "Possible fluctuations in electron streams due to ions," *J. Appl. Phys.*, vol. 19, pp. 231–236; 1948.
[5] A. V. Haeff, "The electron-wave tube," Proc. IRE, vol. 37, pp. 4–10; January, 1949.
[6] J. R. Pierce and W. B. Hebenstreit, "New type of high-frequency amplifier," *Bell Sys. Tech. J.*, vol. 28, pp. 33–51; 1949.
[7] D. H. Looney and S. C. Brown, "The excitation of plasma oscillations," *Phys. Rev.*, vol. 93, pp. 965–969; 1954.
[8] E. I. Gordon, "Plasma Oscillations, Interactions of Electron Beams with Gas Discharge Plasmas," Ph.D. dissertation, Mass. Inst. Tech., Cambridge; 1957.
[9] G. Wehner, "Plasma oscillator," *J. Appl. Phys.*, vol. 21, pp. 62–63; 1950.
[10] M. J. Kofoid, "Experimental two-beam excitation of electron oscillations in a plasma without sheaths," *Phys. Rev. Lett.*, vol. 4, pp. 556–557; 1960.

perpendicular to the direction of the beam and the effective beam boundaries were neglected; *i.e.*, the problem was considered one-dimensional.

4) Thermal velocities and collisions of the plasma electrons were neglected.
5) The plasma and the beam were assumed spatially uniform.

One may interpret this dispersion relation as giving either the propagation constant γ of waves whose frequency is ω, or the frequency of oscillation of disturbances whose wave number is γ. It is the former interpretation which we employ in this paper.

In the absence of a secondary electron beam or alternative feedback path, we expected the system of an electron beam interacting with a plasma over a finite length to be inherently stable; that is, we did not expect spontaneous oscillations.[11] On the other hand, small perturbations in current (shot noise) or velocity of the incoming electron beam or fluctuations arising in the plasma would increase in amplitude along the electron beam. In the first[12] of the two experiments described below (Fig. 1) we deliberately introduced a modulation of the electron beam at a microwave frequency and observed the amount by which this modulation was increased after having passed through the plasma. This experiment verified some of the early predictions. Kharchenko, *et al.*,[13] examined the modulation of the beam as it emerged from the plasma when no microwave modulation had been applied initially. They found a noise modulation whose frequency spectrum was sharply peaked at the plasma frequency, presumably due to the selective amplification of wide band fluctuation noise. Finally, Bogdanov,[14] and very recently, Allen and Kino,[15] repeated our first experiment with a longitudinal magnetic field and observed several interesting new effects.

During the course of the first experiment it was shown[16] that a cylindrical plasma column was capable of supporting electrostatic waves whose velocity could be made slow compared with the velocity of light. This suggested the second experiment[17] described below (Fig. 4) in which traveling-wave interaction occurred between such a slow wave and an electron beam which passed down the axis of the plasma at a velocity about equal to the wave velocity.

II. Interaction at Plasma Resonance

The first experiment utilized devices of the type shown in Fig. 1. An electron beam was modulated by a short helix, passed along the axis of the plasma column, and then upon emerging was demodulated by a second helix. The plasma density could be varied by changing the arc current, and strong amplification was found to occur[12] only when the plasma frequency was very close to the modulation frequency.

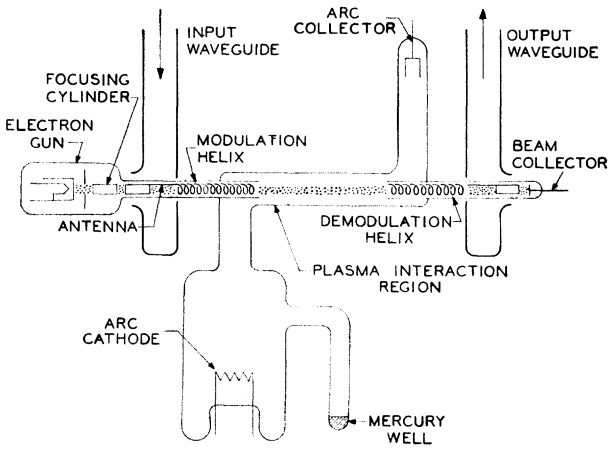

Fig. 1—Helix modulation experiment.

A. The Effect of Thermal Velocities of the Plasma Electrons—One-Dimensional Theory

Bohm and Gross[3] have derived the dispersion equation, including the effect of the thermal distribution of velocities of the plasma electrons, for a broad electron beam passing through a stationary plasma. The effect of short-range collisions of the plasma electrons may also be included in an approximate manner through the introduction of a velocity-independent collision frequency[18] ν. We now give a discussion of the solutions of this equation for the conditions of our first experiment.

All waves were assumed to have exponential spatial and time dependence $e^{i(\omega t-\gamma z)}$, where $\gamma=\beta-i\alpha$ was the complex propagation constant and α and β were both real. A beam plasma frequency was defined in terms of the beam electron density n_b by $\omega_b^2=n_be^2/m\epsilon_0$. The thermal distribution of velocities of the electron beam about their mean velocity v_b was neglected since their

[11] P. A. Sturrock, "Excitation of plasma oscillations," *Phys. Rev.*, vol. 117, pp. 1426–1429; 1960.

[12] G. D. Boyd, L. M. Field, and R. W. Gould, "Excitation of plasma oscillations and growing plasma waves," *Phys. Rev.*, vol. 109, pp. 1393–1394; 1958. (This article contains a preliminary account of the first experiment described here.)

[13] I. F. Kharchenko, *et al.*, "Experimental and theoretical investigation of the interaction of an electron beam with a plasma," *Proc. Conf. on Ion Phenomena in Gases*, Uppsala, Sweden, vol. II, pp. 671–680; 1959.

[14] E. V. Bogdanov, V. J. Kislov, and Z. S. Tchernov, "Interaction between an electron stream and a plasma," *Proc. Symp. on Millimeter Waves*, Polytechnic Inst. of Brooklyn, N. Y., vol. 9, pp. 57–71; April, 1959.

[15] M. A. Allen and G. S. Kino, "Interaction of an electron beam with a fully ionized plasma," *Phys. Rev. Lett.*, vol. 6, pp. 163–165; 1961.

[16] A. W. Trivelpiece, "Slow Wave Propagation in Plasma Waveguides," Ph.D. dissertation, Calif. Inst. Tech., Pasadena; 1958. Also, A. W. Trivelpiece and R. W. Gould, "Space charge waves in cylindrical plasma columnes," *J. Appl. Phys.*, vol. 30, pp. 1784–1793; 1959. Also, "Electro-mechanical modes in plasma waveguides," *Proc. IEE*, vol. 105, pt. B, pp. 516–519; 1958.

[17] G. D. Boyd and R. W. Gould, "Travelling wave interaction in plasmas," *J. Nuclear Energy*, vol. 2, pt. C, pp. 88–89; 1961. (This article contains a preliminary account of the second experiment described here.)

[18] R. W. Gould, "Plasma Oscillations and Radio Noise from the Disturbed Sun," Calif. Inst. of Tech., Pasadena, Calif., Tech. Rept. 4, Contract NONR 220 (13); September, 1955.

random energy of approximately 0.1 ev was small compared to the random energy of 4.7 ev of the plasma electrons.

With these definitions the one-dimensional dispersion relation may be written

$$1 = \omega_p^2 \frac{(\omega - i\nu)}{\omega} \int_u \frac{f_0(u)du}{(\omega - \gamma u_z - i\nu)^2} + \frac{\omega_b^2}{(\omega - \gamma v_b)^2}, \quad (4)$$

where $f_0(u)$ was the normalized unperturbed distribution function of velocities of the plasma electrons and $du = du_x du_y du_z$. We assumed a Maxwellian velocity distribution

$$f_0(u) = \left(\frac{m}{2\pi kT}\right)^{3/2} \exp\left\{-\frac{m}{2kT}(u_x^2 + u_y^2 + u_z^2)\right\}, \quad (5)$$

where T is the equivalent "temperature" of the plasma electrons, and u is their random velocity vector.

The integral which resulted when (5) was substituted into (4) may be expressed in terms of the error function of complex argument. A large-argument asymptotic expansion of this function was easily obtained by expanding the denominator of the integral in (4) in powers of $\gamma u_z/(\omega - i\nu)$ and integrating term by term. The dispersion relation became

$$1 = \frac{(\omega_p/\omega)^2}{1 - i\frac{\nu}{\omega}}\left\{1 + \frac{\Gamma^2}{R\left(1 - i\frac{\nu}{\omega}\right)^2} + \frac{5}{3}\frac{\Gamma^4}{R^2\left(1 - i\frac{\nu}{\omega}\right)^4} + \cdots\right\} + \frac{(\omega_b/\omega)^2}{(\Gamma - 1)^2}, \quad (6)$$

where

$$R = \frac{mu_b^2}{3kT}. \quad (7)$$

is the ratio of the beam energy to the mean energy of a plasma electron and

$$\Gamma = \frac{\gamma v_b}{\omega} \quad (8)$$

is a normalized propagation constant. For the first experiment $R \approx 100$ and $|\Gamma| \approx 1$.

Neglecting collisions, there was a range of frequencies for which Γ was complex and a range for which it was real. Since $R \gg 1$, only the first two terms of the above series were considered. Eq. (6) then reduced to

$$(\Gamma - 1)^2(\Gamma^2 + \Lambda) + \sigma = 0, \quad (9)$$

where

$$\sigma = R\left(\frac{\omega_b}{\omega_p}\right)^2, \qquad \Lambda = R\left(1 - \frac{\omega^2}{\omega_p^2}\right) \quad (10)$$

Fig. 2 shows the locus of the roots of this equation in the complex Γ plane with Λ and σ as parameters. The growth constant is $-\alpha = (\omega/v_b)$ Im Γ. Alternatively, the gain is -8.68α db per cm, if α has units cm^{-1}. For a growing wave α is negative. This figure reveals that the maximum growth rate α occurs when the frequency ω is within a few per cent of the plasma frequency, provided $0.003 \leq \sigma \leq 3.0$ and $R \geq 30$. Thus maximum interaction occurs close to plasma resonance. In Fig. 3 we plot the normalized growth rate vs ω_p^2/ω^2 for representative beam energies (R) and beam densities (ω_b^2/ω_p^2).

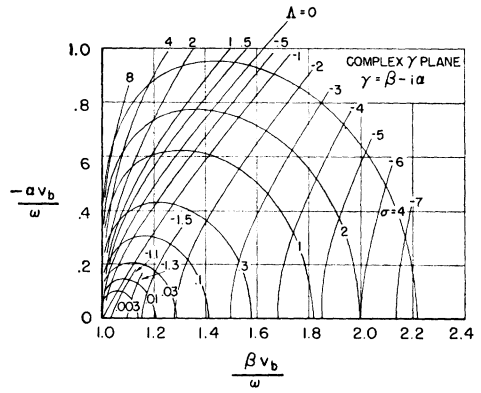

Fig. 2—Solution of (9) for the complex propagation constant

$$\Gamma = \frac{\gamma v_b}{\omega} = \frac{\beta v_b}{\omega} - i\frac{\alpha v_b}{\omega}$$

over a range of values of the parameters σ and Λ.

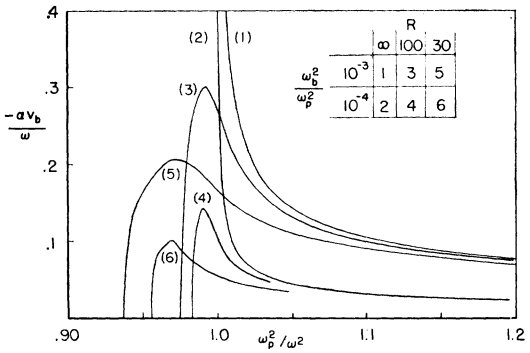

Fig. 3—Growth parameter $-\alpha$ vs the normalized plasma frequency squared. R is the ratio of the electron-beam energy to the average random energy of the plasma electrons. ω_b^2/ω_p^2 is the ratio of the beam-electron density to the plasma-electron density.

The effect of collisions is to reduce the growth rate, and it is convenient to evaluate this effect when $\omega = \omega_p$ ($\Lambda = 0$) since this is the condition for maximum growth rate (approximately). If it is also assumed that collisions are infrequent ($\nu \ll \omega$), (6) may be written as

$$\Gamma = 1 + i\sqrt{\frac{\sigma}{\Gamma^2 + iR\frac{\nu}{\omega}}}. \quad (11)$$

This equation is easily solved by iteration, taking Γ^2 equal to unity on the right-hand side as the first step. (Results are given in Tables I and II of Sections V and VI.)

B. The Effect of Finite Electron-Beam Diameter

In the Appendix we derive the dispersion equation for waves which can exist upon an electron beam of radius b passing through an infinite plasma. Thermal velocities and collisions of the plasma electrons are neglected. It is shown that the effect of the finite beam diameter is to introduce a beam-plasma reduction factor into (3), so that it can be written as

$$1 = \frac{\omega_p^2}{\omega^2} + \frac{(\omega_b')^2}{(\omega - \gamma v_b)^2} \tag{12}$$

where

$$\left(\frac{\omega_b'}{\omega_b}\right)^2 = \frac{1}{1 + \dfrac{I_0(\gamma b)K_1(\gamma b)}{I_1(\gamma b)K_0(\gamma b)}} . \tag{13}$$

In the thin beam limit ($\gamma b \to 0$), the above becomes

$$\left(\frac{\omega_b'}{\omega_b}\right)^2 \simeq \frac{1}{2}(\gamma b)^2(0.11593 - \ln \gamma b) \qquad \gamma b \ll 1, \tag{14}$$

which is similar to that obtained by Sturrock.[11]

We note from (13) that, if γ is real, the effect of finite beam size is simply to reduce the effective beam density and hence the rate of growth. When the growth per wavelength is small ($-\alpha \ll \beta$), it is sufficient to evaluate (13) by setting $\gamma = \omega/v_b$. Fig. 3 shows that this is not always a good approximation, and a complete discussion of the solutions of (12) and (13) has not been given. The solutions of the corresponding dispersion equation which results when the beam and plasma are subjected to a very strong axial magnetic field is given in Bogdanov, *et al.*[14]

III. Slow-Wave Interaction

During the course of the first experiment (Fig. 1), an interaction of the electron beam with the plasma was obtained when the plasma frequency was several times the modulation frequency imposed on the beam.

In this case the electron beam interacts with one of the slow space-charge waves which propagates along the plasma column. These propagating waves are electromechanical in nature and result from the interplay of kinetic energy of the plasma electrons and the energy stored in the electric field. In the special case of no axial magnetic field these waves are surface waves. They have been studied in detail by Trivelpiece and Gould.[16] Synchronism between an electron beam and such a slow wave results in familiar traveling-wave interaction. (See Pierce and Field[19] for a physical description of traveling-wave interaction.)

The second experiment described in this paper was designed to investigate more completely this traveling-wave interaction. A different configuration, shown in Fig. 4, was employed. In order to enhance the traveling-wave interaction, the diameter of the plasma column was made smaller than in the first experiment, and the electron-beam diameter was made larger. Modulation and demodulation of the electron beam was accomplished with cavity resonators (at a fixed frequency) so as to allow a variable beam velocity.

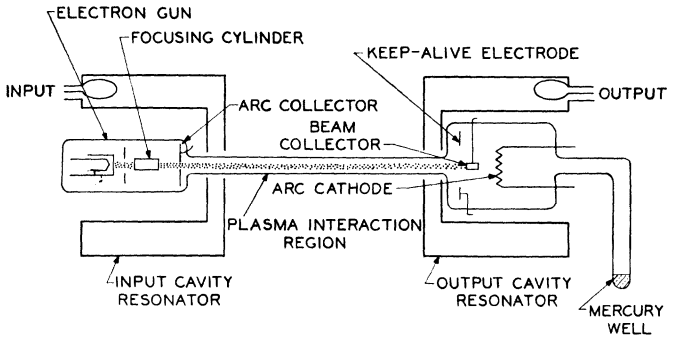

Fig. 4—Cavity-modulation experiment.

A. Slow-Wave Mode of Propagation

We now give a short theoretical discussion of the electrostatic waves which propagate along a nondrifting plasma column of radius a which fills a glass tube whose outer radius is c. Two cases will be considered: 1) a perfectly-conducting surface at radius c, and 2) the glass tube in free space. Thermal velocities and collisions of the plasma electrons will be neglected.

The electric fields of these modes are derivable from a potential if their phase velocity is small compared to the velocity of light.[16] In this approximation the potential satisfies the Laplace equation. First let there be a conducting surface at radius c. Field are assumed to vary as $e^{i(\omega t - n\theta - \beta z)}$. In the absence of the electron beam and neglecting collisions, the propagation constant is real, so β is used for the propagation constant instead of $\gamma(\alpha = 0)$.

The time-varying potential in each region is given by

$$\phi_1 = \frac{I_n(\beta r)}{I_n(\beta a)} e^{i(\omega t - n\theta - \beta z)} \qquad r \leq a$$

$$\phi_1 = \frac{I_n(\beta r)K_n(\beta c) - I_n(\beta c)K_n(\beta r)}{I_n(\beta a)K_n(\beta c) - I_n(\beta c)K_n(\beta a)} e^{i(\omega t - n\theta - \beta z)} \qquad a \leq r \leq c. \tag{15}$$

Matching tangential electric field and normal displacement at $r = a$, and using (2) for the plasma dielectric permittivity and κ as the relative dielectric constant of the glass, one obtains the dispersion equation

$$\left(1 - \frac{\omega_p^2}{\omega^2}\right)\frac{1}{\kappa} = \frac{I_n(\beta a)}{I_n'(\beta a)}\left\{\frac{I_n'(\beta a)K_n(\beta c) - I_n(\beta c)K_n'(\beta a)}{I_n(\beta a)K_n(\beta c) - I_n(\beta c)K_n(\beta a)}\right\}, \tag{16}$$

where the primes denote derivatives of the Bessel functions with respect to the argument. In the limit of

[19] J. R. Pierce and L. M. Field, "Traveling-wave tubes," Proc. IRE, vol. 35, pp. 108–111; February, 1947.

large βa the asymptotic frequency of propagation is

$$\frac{\omega}{\omega_p} = \frac{1}{\sqrt{1+\kappa}}. \tag{17}$$

The solution of this equation for the circularly symmetrical mode ($n=0$) is shown in Fig. 5 by the lower dashed curve, where we plot ω/ω_p vs βa. The phase and group velocities are given by ω/β and $\partial\omega/\partial\beta$, respectively. Angular dependent modes are not of particular interest in the second experiment since their fields vanish on the axis where the electron beam passes and, in addition, the excitation cavities are cylindrically symmetric.

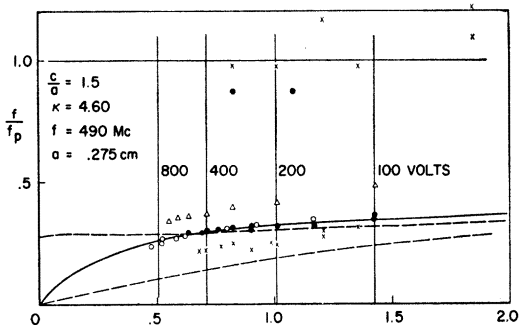

Fig. 5—Frequency vs propagation constant βa for the surface-wave mode of propagation on a plasma-glass column in free space (solid curve), and when covered with a conducting surface (dashed curve). In the latter case, the upper dashed curve represents the $n=1$ mode, and the lower dashed curve represents the $n=0$ mode. The ○, ● and △ correspond to measurements on the plasma-glass column in free space, and should lie on the theoretical solid curve. The × data was obtained with the glass coated with a conducting layer, and such points should lie on the lower dashed curve.

Where the glass tube is in free space rather than being surrounded by a metallic conductor, expressions for the potential in three separate regions—1) plasma $r \leq a$, 2) glass $a \leq r \leq c$, 3) free space $c \leq r < \infty$—must be joined so that the tangential field and normal displacement are continuous. This leads to a dispersion equation for the circularly symmetric mode ($n=0$)

$$\left(1 - \frac{\omega_p^2}{\omega^2}\right)\frac{I_1(\beta a)}{I_0(\beta a)} = \frac{-\kappa}{be\coth(\beta c, \beta a)} \cdot \frac{\kappa + \dfrac{K_1(\beta c)}{K_0(\beta c)}\dfrac{1}{be\tanh(\beta c, \beta a)}}{\kappa + \dfrac{K_1(\beta c)}{K_0(\beta c)}Be\tanh(\beta c, \beta a)}, \tag{18}$$

where the functions

$$be\coth(\beta c, \beta a) = \frac{I_1(\beta c)K_0(\beta a) + I_0(\beta a)K_1(\beta c)}{I_1(\beta c)K_1(\beta a) - I_1(\beta a)K_1(\beta c)}$$

$$be\tanh(\beta c, \beta a) = \frac{I_1(\beta c)K_1(\beta a) - I_1(\beta 1)K_1(\beta c)}{I_0(\beta c)K_1(\beta a) + I_1(\beta a)K_0(\beta c)}$$

$$Be\tanh(\beta c, \beta a) = \frac{I_0(\beta c)K_0(\beta 1) - I_0(\beta a)K_0(\beta c)}{I_1(\beta c)K_0(\beta a) + I_0(\beta a)K_1(\beta c)} \tag{19}$$

are defined and tabulated by Birdsall.[20] Solution of this equation is depicted by the solid line in Fig. 5. The horizontal line in Fig. 5 at $\omega/\omega_p=1$ corresponds to plasma oscillations which are independent of the wavelength of the disturbance.

The vertical lines labeled 800, 400, 200, and 100 volts correspond to constant phase velocity lines when the frequency is fixed and the plasma density is varied. The intersection of these curves with any of the propagation constant curves specifies the operating point at which the electron beam velocity is synchronous with the phase velocity of the surface wave.

B. *Interaction Impedance*

An electron beam traveling in synchronism with the slow surface wave will interact with the axial electric field of the wave. Under these conditions a spatially growing wave will result (the propagation constant becomes complex), so that the RF energy traveling along the plasma column increases with distance. This energy is supplied by the conversion of the beam kinetic energy.

Pierce[21] has shown that an approximate value of the growth constant in a traveling-wave amplifier can be expressed in terms of an *interaction impedance*, which is proportional to the square of the axial electric field at the position of the beam per unit power flow in the slow wave. Calculations[22] of this impedance for the circularly symmetric mode of the plasma-glass column in free space (ω-β diagram is given by the solid curve of Fig. 5) are approimately 800 ohms in the range $0.5<\beta a<1.5$.

IV. Characteristics of the Plasma and the Electron Beam

A. *Mercury Arc Discharge*

The positive column of an arc discharge in mercury vapor was the plasma. The mercury gas pressure was regulated by maintaining the temperature of the mercury "well" at 300 ± 0.1°K. The vapor pressure at this temperature was 2.1×10^{-3} mm Hg (2.1 microns), and the density of mercury atoms was 6.8×10^{13} per cm^3. The electron density n_0, corresponding to an electron plasma frequency of 3000 Mc, was 1.12×10^{11} per cm^3. The random energy of the plasma electrons was characterized by an equivalent temperature T_e. Measurements of T_e by Langmuir probes gave $T_e=35{,}000$°K, or 4.7 electron volts. The energy corresponding to the axial drift velocity which is necessary to carry the discharge current was about 0.2 ev and was therefore small compared with the random energy. The collision

[20] C. K. Birdsall, "Memorandum for File ETL-12," Hughes Aircraft Co., Malibu, Calif.; July 1, 1953.

[21] J. R. Pierce, "Traveling Wave Tubes," D. Van Nostrand Co., New York, N. Y.; 1950.

[22] G. D. Boyd, "Experiments on the Interaction of a Modulated Electron Beam with a Plasma," Ph.D. dissertation, Calif. Inst. Tech., Pasadena; 1959. Also, "Power Flow and Gap Coupling to Slow Wave Plasma Modes," Electron Tube and Microwave Lab., Calif. Inst. Tech., Pasadena, Tech. Rept. 12, NONR 220 (13); June, 1959.

frequency of plasma electrons with the sheath at the tube wall was approximately 129×10^6 sec^{-1} for a plasma column diameter of 1.04 cm (as in the first experiment). The collision frequency of electrons with un-ionized mercury atoms was 37×10^6 sec^{-1} corresponding to a mean-free path of the plasma electrons through mercury atoms of approximately 3.5 cm, which was somewhat greater than the tube diameter.

The mean-free path for beam electrons of 100 to 1000 volts in the plasma ranged from about 26 to about 65 cm at the vapor pressure used throughout these experiments.

B. Electron Beam

The electron-beam gun was of the conventional type used in traveling-wave tubes. Beam focusing was possible with an electron lens (focusing cylinder, Figs. 1 and 4) and ion space-charge forces. *L* cathodes were found to be the most satisfactory in resisting the adverse effects of mercury ion bombardment. Arcing between gun electrodes due to the presence of ions did not seem to occur in the voltage range employed. The cathode button diameters were 0.045 and 0.090 inch in the helix modulation tube of Fig. 1 and in the cavity modulation tube of Fig. 4, respectively.

V. Helix Modulation Experiment

A. Interaction at Plasma Resonance

A schematic of the helix modulation tube is shown in Fig. 1. The plasma interaction length between helices was about 5 cm. The inner radius of the glass tube was 0.52 cm. The *S*-band coupling waveguides were tapered to 1 cm in height. The input and output helices were each 3 cm long. The helix-synchronous voltage was 400 volts.

In the operation of the experiment the electron beam was modulated with a microwave frequency between 2.2 and 4.0 kMc, and the output signal from the demodulation helix was observed as the arc current was swept. The plasma density, and thus the square of the plasma frequency, is approximately proportional to arc current in low-pressure arc discharges.[23] According to the theory presented in Section II, the output signal level should be a maximum when the arc current is such that plasma frequency ω_p equals the modulation frequency ω. This value of arc current for maximum interaction should change as the input frequency is changed. For convenience, the arc current was swept at a 60-cps rate, so that the result could be displayed on an oscilloscope.

The output signal level was displayed on the *y* axis of the oscilloscope, while a signal proportional to the discharge current was used to drive the *x* axis. Fig. 6 shows the resulting display for six different modulating frequencies. The arc current zero line is the heavy vertical line on the extreme left. From these and similar traces the current for maximum interaction was obtained, and the result is shown in Fig. 7.

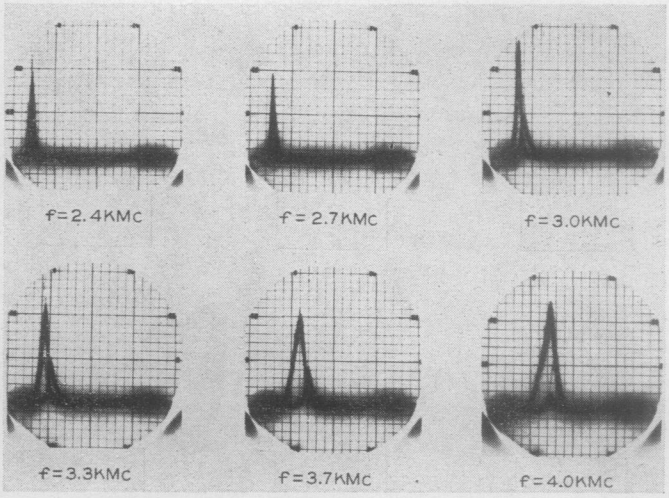

Fig. 6—Detected output signal vs arc current as obtained from the helix-modulation tube. Horizontal calibration: 20 divisions equal 0.40 ampere.

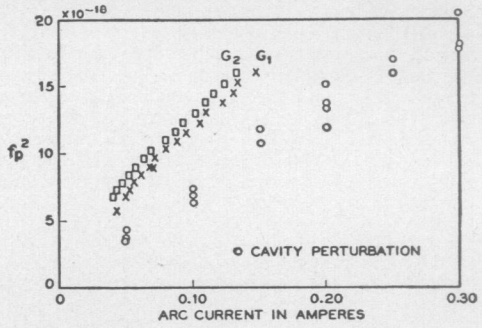

Fig. 7—G_1 and G_2 give the axial plasma frequency squared as obtained from Fig. 6. The circles represent measurements of the average plasma frequency squared over the plasma interaction region as obtained by the cavity perturbation method.

The observation that points G_1 and G_2 lie on relatively straight lines passing nearly through the origin is strong evidence that the interaction observed corresponds to plasma resonance. Approximate equality of the modulation frequency and the plasma frequency must be ascertained from an independent measurement of plasma density. The fact that the straight lines when extrapolated to zero frequency do not pass exactly through the origin may be explained in terms of part of the plasma being produced by beam collisions. Differences in beam focusing probably accounts for the difference between the intercepts of curves G_1 and G_2, taken with different electrode potentials.

To obtain a measurement of electron density by an independent method, the cavity-perturbation tech-

[23] B. Klarfeld, "Characteristics of the positive column of gaseous discharge," *J. Phys. USSR*, vol. 5, pp. 155–175; 1941.

nique[24–26] which measured the average plasma electron density over the cross section, was applied to the plasma interaction region of the helix tube. The average square of plasma frequency was also plotted vs arc current in Fig. 7. The difference in slopes (a factor of 1.4) between the cavity data and G_1 or G_2 may be explained by the fact that electron density on the axis, where interaction occurs, is higher than the average density for a specific current. Assuming a parabolic dependence of density on radius,[27] it was estimated from the ratio of the slopes that the edge plasma density was about 0.4 of the plasma density on the axis, which was in reasonable accord with Klarfeld.[23]

B. Rate of Growth

Table I presents theoretical growth constants in db per cm for different values of the electron-beam current. All rates of growth are for 3000 Mc, assume a 400-volt beam, include a beam-reduction factor of 0.4 [from (25)], a beam diameter of 3 mm, and a value of $R=100$. The first column gives the maximum rate of growth (such as that taken from the peak of the curves in Fig. 3) and neglects collisions. The second column also neglects collisions and gives the growth at the plasma frequency $\omega=\omega_p$. The remaining columns are also for $\omega=\omega_p$, but include collision frequencies ν of 30, 100, and 300 Mc, respectively.

TABLE I

THEORETICAL GROWTH CONSTANTS AT PLASMA RESONANCE FOR THE HELIX MODULATION TUBE

I_b	Max G db per cm	G at $\omega=\omega_p$ db per cm			
ma	$\nu=0$	$\nu=0$	$\nu=30\times10^6$	$\nu=100\times10^6$	$\nu=300\times10^6$
0.25	17.2	11.1	10.74	9.68	6.95
0.5	22.05	15.5	14.93	13.4	9.71
1.0	27.55	21.4	20.55	18.38	13.5
2.0	34.0	29.2	27.9	24.96	18.68

Experimentally, the maximum net gain observed between the input and output waveguides was about +25 db. Under this condition the cathode current was 2.0 ma, and the current reaching the beam collector was 0.48 ma. When the arc was turned off but the beam left on, the net loss between waveguides was as little as 10 db if the beam remained well focused. This implies an electronic gain of 35 db in the 5-cm interaction length or a growth constant of 7 db per cm. The theoretical prediction, assuming a beam current of 0.5 ma and a collision frequency of 100 Mc (Table I), was about 13.4 db per cm. On many occasions the helix modulation tube showed a net *loss* of 10 db or so. Adjusting electrode potentials of the device so as to show net gain was sometimes difficult.

The theoretical bandwidth of this amplification device is less than 1 per cent. The experimentally observed bandwidths of 25 per cent or so seen in Fig. 6, together with the reduced gains, are likely to be explained by the variations in the plasma density *along* the path of the beam. When the plasma frequency varies along the path of the electron beam, it can be shown that the effect is to reduce the gain at any one frequency and to increase the range of frequencies over which amplification is possible. The density is probably lowest where the beam enters and where it emerges because of diffusion losses.

It is difficult, for two reasons, to observe the growing waves at plasma resonance by moving an antenna along the outside of the glass column. First, the fields decay exponentially away from the surface of the beam and the decay factor is large, since $\beta a=8.2$ for the helix tube at 3000 Mc and 400 volts. Secondly, as may be seen from the following argument, plasma oscillations ($\omega=\omega_p$) produce very little field outside the plasma column. The dielectric constant (2) is zero in the plasma, and hence the normal component of the displacement vector vanishes at the edge of the plasma. Therefore, the normal component of the electric field vanishes outside the plasma column. Of course this argument neglects the effect of random energy of the plasma electrons, but it does serve to indicate that the field outside should be small. The first argument does not apply to the cavity modulation tube to be discussed in Section VI, since βa is approximately unity and the electron beam passes closer to the edge of the plasma column in that tube. The growing wave at plasma resonance *was* detectable in the cavity modulation tube using a traveling probe.

C. Slow-Wave Interaction

When the electron beam was defocused so badly that it filled most of the plasma column, being reflected from the sheath from the edge of the plasma column and then partially collected at the second helix, an interaction was observed when the plasma frequency was greater than the modulation frequency. Fig. 8 shows the detected output signal vs arc current. The arc current increases from left to right and is zero at the heavy vertical line at the far left. Two interactions may be seen, the one at lower current occurring when

[24] M. A. Biondi and S. C. Brown, "Measurements of ambipolar diffusion in helium," *Phys. Rev.*, vol. 75, pp. 1700–1705; 1949.
[25] K. B. Persson, "Limitations of the microwave cavity method of measuring electron densities in a plasma," *Phys. Rev.*, vol. 106, pp. 191–195; 1957.
[26] S. J. Buchsbaum and S. C. Brown, "Microwave measurements of high electron densities," *Phys. Rev.*, vol. 106, pp. 196–199; 1957.
[27] R. M. Howe, "Probe studies of energy distributions and radial potential variations in a low pressure mercury arc," *J. Appl. Phys.*, vol. 24, pp. 881–894; 1953.

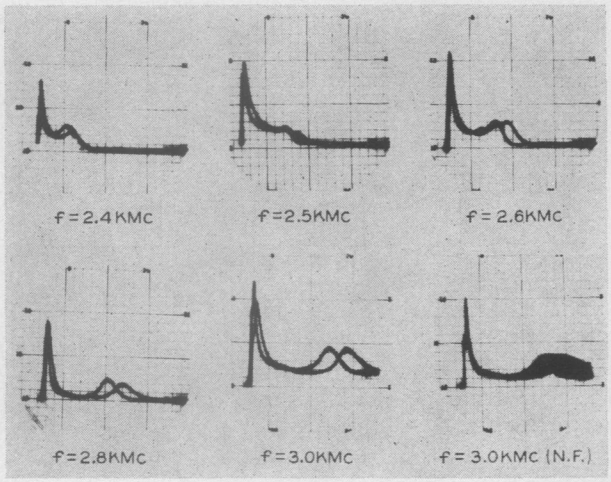

Fig. 8—Detected output signal vs arc current as obtained from the helix tube. Calibration as in Fig. 6. The interaction peak at the larger current is with the surface wave mode of propagation. NF is with the output unfiltered.

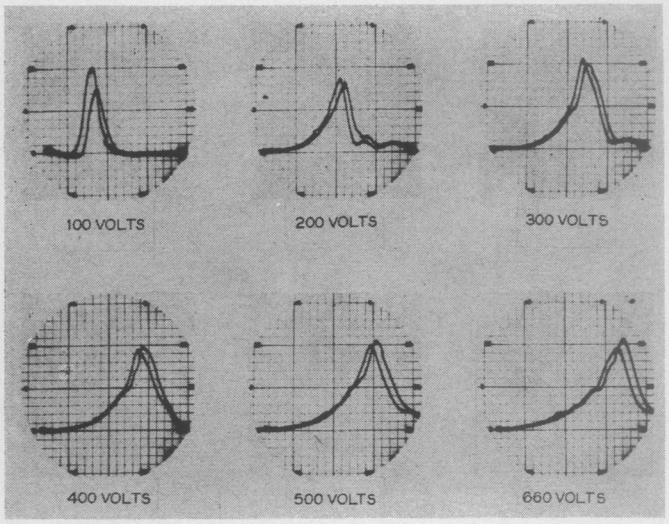

Fig. 9—Detected output signal vs arc current as obtained from the cavity-modulation tube. Horizontal calibration: 20 divisions equal 0.050 ampere. The beam is interacting with the angularly independent surface-wave mode of propagation.

$\omega_p = \omega$, and the one at higher current presumably due to the axially symmetric surface wave mode of propagation. The subsidiary maxima in Fig. 2 of the preliminary report[12] were probably also due to the surface-wave interaction. If the beam were not deliberately defocused, interaction with the surface wave could not be observed since the fields are strong only at the surface of the plasma column.

Also shown in Fig. 8 are two photographs at the same frequency taken with the detected output signal both filtered and nonfiltered (NF). Appreciable noise is present in both interactions, some of which may be associated with moving striations.[28]

In Figs. 6, 8 and 9 hysteresis is evident. This may be due to space-charge buildup and decay or to nonequilibrium heating effects. The hysteresis phenomena is not completely understood.

VI. Cavity Modulation Experiment

A. Slow-Wave Interaction

A larger beam and smaller plasma column were necessary to obtain strong interaction with the surface-wave mode of propagation, thus the device shown in Fig. 4 was constructed. By varying the beam voltage (approximately 1000 to 100 volts) βa could be made to fall between 0.5 and 1.5. By operating with a significantly smaller value of βa than in the helix tube, the surface-wave fields are much stronger near the axis where the electron beam passes. By employing an axial magnetic field it would be possible to have the fields on the axis stronger than at the surface.[16]

The detected output signal 490 Mc is shown in Fig. 9 vs arc current at six different electron-beam voltages. The zero of current is the numbered heavy line at the far left. As the beam velocity increases, the phase velocity of the slow surface wave must also increase to fulfill the synchronism condition. From Fig. 5 it is seen that βa and f/f_p decrease as the velocity increases. Thus as the beam velocity increases the plasma frequency must increase if synchronism is to be maintained. Fig. 9 shows that, indeed, as the beam voltage is increased, the arc current for maximum gain increases.

The electron density in the plasma column of the cavity-modulation tube was measured by the cavity-perturbation technique.[24–26] as a function of arc current. From the arc current corresponding to the peak interaction in Fig. 9 one may obtain the *experimental* ω-β diagram as shown by the data points in Fig. 5. The result is seen to correspond well to the theoretical curves. Any errors in the cavity measurements of plasma density would tend to shift the vertical scale.

Interaction was also observed at the plasma resonance with the cavity tube. This interaction occurred near the value of the current at which the arc extinguished, and stable operation was difficult. Nevertheless, the values of the interaction-arc current at which this interaction occurred were used to determine the plasma frequency $f_p = \omega_p/2\pi$, and the results (f/f_p) are plotted in Fig. 5 near the horizontal line at $f/f_p = 1$.

B. Growing Surface Waves

The surface-wave fields are strongest at the surface of the plasma column. A traveling probe at the surface of the glass column was used to detect a growing standing-wave pattern (Fig. 10). The standing-wave pattern is a result of the interference between the growing surface wave and the wave which is reflected by the output cavity resonator. From the standing-wave pattern one may measure the electronic wavelength on the plasma column. This is in agreement with the value predicted from the beam voltage.

[28] L. Pekarek, "Theory of moving striations," *Phys. Rev.*, vol. 108, pp. 1371–1372; 1957.

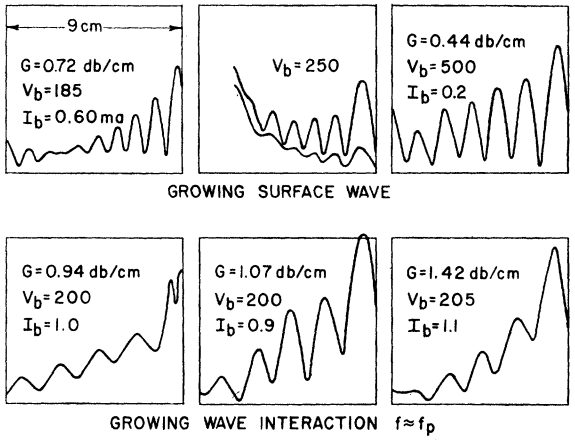

Fig. 10—Growing wave strength vs distance as obtained by a traveling probe at the surface of the glass column of the cavity-modulation tube.

The 250-volt case in Fig. 10 is of particular interest. The lower curve was taken with the beam current greatly reduced by lowering the cathode temperature. The signal then decayed along most of the interaction region because of collisional attenuation in the surface-wave propagation. The upper curve is with a normal beam current and shows a growing wave.

Theory[21] predicts a growth constant of 2.75 db per cm when an interaction impedance of 800 ohms (Section III-B) and a 200-volt beam at 1-ma current are assumed, and when space charge in the beam, plasma random energy, and collisions are neglected. A representative experimental value at 1 ma and 200 volts is about 0.8 db per cm. The discrepancy between the theoretical and experimental growth constants may be due possibly to the neglect of loss along the plasma column in the theoretical calculation.

C. Interaction at Plasma Resonance

Because of the smaller value of βa (approximately 1) for the cavity tube (as compared with $\beta a \approx 8$ in the helix tube), it was found that a growing standing-wave pattern could be observed with a traveling probe outside the plasma column (see Fig. 10). A representative growth constant was found to be 1 db per cm at 1-ma beam current.

Measurements on the growing standing-wave pattern indicated that the interfering wave had a large phase velocity compared to the forward-beam velocity, and thus the standing-wave pattern was probably due to stray radiation in free space from the signal source. The standing-wave pattern could not have been a result of the reflected surface wave since the latter does not propagate when $f=f_p$.

Table II gives theoretical growth constants in db per cm, assuming a 200-volt beam, a beam reduction factor of 0.21 from (25) a beam diameter of 4.8 mm, and a value of $R=200/4.7=42.6$. The presentation of the data is similar to that in Table I.

TABLE II

THEORETICAL GROWTH CONSTANTS AT PLASMA RESONANCE FOR THE CAVITY-MODULATION TUBE

I_b	Max G db per cm	G at $\omega=\omega_p$ db per cm			
ma	$\nu=0$	$\nu=0$	$\nu=30\times10^6$	$\nu=100\times10^6$	$\nu=300\times10^6$
0.25	6.61	5.32	4.72	3.58	2.11
0.5	8.27	7.23	6.38	4.92	2.96
1.0	10.32	9.62	8.52	6.70	4.16
2.0	12.72	12.52	11.20	9.05	5.78

The experimentally measured growth rate of 1 db per cm was considerably less than the theoretical value of about 6.7 db per cm (assuming 100-Mc collision frequency), and this discrepancy is most likely due to variations of the axial plasma density or to an incorrect estimate of the beam diameter in the plasma.

VII. SUMMARY AND CONCLUSIONS

Experiments have been performed substantiating two types of interaction between a modulated electron beam and a plasma. In one case the plasma acts as a resonant, nonpropagating medium and in the other as a slow traveling-wave structure with which synchronism between it and the electron beam is observed.

Exponential growth constants along the beam were measured with a traveling probe for both interactions. The experimental rates of growth were considerably less than that predicted theoretically. For the traveling-wave interaction, the neglect of loss and the random energy of the plasma electrons in the theory are probably of most importance.

Trivelpiece and Gould[16] have shown that immersing the plasma column in an axial magnetic field converts the nonpropagating plasma resonance into a backward-wave propagating mode (phase and group velocities in opposite directions) with which backward-wave interaction (and thus oscillation) is possible. Recently Targ and Levine[29] have observed such backward-wave oscillations. Structureless slow-wave propagating circuits are intriguing and deserve further investigation.

APPENDIX

THREE-DIMENSIONAL THEORY NEGLECTING THE RANDOM ENERGY OF THE PLASMA ELECTRONS

If in a plasma the wavelength of the disturbance is small compared to the free-space wavelength at that frequency, the magnetic field associated with plasma oscillations may be neglected. Under this quasi-static approximation the time-varying potential and charge

[29] R. Targ and L. P. Levine, "Backward-wave microwave oscillations in a system composed of an electron beam and a hydrogen gas plasma," *J. Appl. Phys.*, vol. 32, pp. 731–737; 1961.

density are related by Poisson's equation

$$\nabla^2\phi_1 = -\rho_1/\epsilon_0. \tag{20}$$

In the one-dimensional case analyzed in Section II-A the quasi-static *approximation* is unnecessary since the time-varying magnetic field vanishes identically ($\nabla\times\boldsymbol{E}_1 = -\gamma\boldsymbol{e}_z\times\boldsymbol{E}_1 = 0$).

The three-dimensional problem considered here consists of an electron beam of finite radius b passing through a nondrifting infinite cold plasma. To obtain the dispersion equation for growing waves, one computes the sum of the ac charge densities of the beam and of the plasma from the linearized small-signal continuity and force equations. Substituting this sum into (20) and rewriting slightly, one obtains

$$\nabla\cdot\left\{1 - \frac{\omega_p^2}{\omega^2} - \frac{\omega_b^2}{(\omega - \gamma v_b)^2}\right\}\nabla\phi_1 = 0, \tag{21}$$

where a z dependence of $e^{-i\gamma z}$ has been assumed. This is the appropriate differential equation for the beam and plasma together. In the region outside the beam the same equation can be used by setting $\omega_b = 0$.

Note that (21) is written in the form $\nabla\cdot\boldsymbol{D}_1 = 0$, where $\boldsymbol{D}_1$ is the displacement vector. In this form the boundary condition at the interface between the region containing plasma alone and that containing plasma plus beam is evident: the normal component of the quantity $\boldsymbol{D}_1$ is continuous between regions. The potential must also be continuous.

The solutions to (21) are either

$$1 = \frac{\omega_p^2}{\omega^2} + \frac{\omega_b^2}{(\omega - \gamma v_b)^2} \qquad r \leq b, \tag{22}$$

or

$$\nabla^2\phi_1 = 0 \qquad 0 \leq r \leq \infty. \tag{23}$$

Eq. (22) is identical to (3). This represents the one-dimensional solution and is independent of beam radius. Eq. (22) was derived by Pierce,[4] except that he was considering the interaction of beam electrons with ions. The solution of this equation is plotted in Fig. 3 under the designation of $R = \infty$.

For the three-dimensional case the solutions are obtained from (23). Note that (23) implies that $\rho_{1b} + \rho_{1p} = 0$, and therefore that the system consisting of the electron beam and the plasma has no density modulation; only a "rippled boundary" form of modulation at $r = b$ which is the interface between the two regions.

Circularly symmetric solutions of (23) contain modified Bessel functions and are, respectively, $I_0(\gamma r)e^{-i\gamma z}$ and $K_0(\gamma r)e^{-i\gamma z}$ for the radius less than or greater than the beam radius. The potential has been taken to be finite at the origin and zero at infinity. Matching the above boundary conditions results in

$$1 = \frac{\omega_p^2}{\omega^2} + \frac{(\omega_b')^2}{(\omega - \gamma v_b)^2}, \tag{24}$$

where

$$\left(\frac{\omega_b'}{\omega_b}\right)^2 = \frac{1}{1 + \dfrac{I_0(\gamma b)K_1(\gamma b)}{I_1(\gamma b)K_0(\gamma b)}}. \tag{25}$$

The only quantitative effect in (24) compared to (3), which neglects the random energy of the plasma electrons, is to replace the electron-beam plasma frequency by a *reduced*-beam plasma frequency ω_b'. This is a result of the difference between *rippled boundary* modulation and density modulation.

Inclusion of the effects of the random energy of the plasma electrons into the finite geometry problem is more difficult due to the complexity of the boundary conditions. As an approximation to the three-dimensional problem it is assumed that one may take the one-dimensional dispersion relation (6) and replace the beam plasma frequency by the reduced-beam plasma frequency of (25). This results in an approximate dispersion relation, including the random energy and collisions of the plasma electrons, for a finite diameter beam in an infinite plasma.

If the electron beam were immersed in a finite axial magnetic field both rippled boundary and density modulation would occur.

Acknowledgement

A great deal of credit for the success of these experiments is attributable to A. F. Carpenter, whose skill and patience in the fabrication of the glass tubes is gratefully acknowledged. Fruitful discussions were enjoyed with Dr. A. W. Trivelpiece.

The continuing support of the Office of Naval Research is very gratefully acknowledged.